An Improved Nonlinear Dynamic Inversion Method for Altitude and Attitude Control of Nano Quad-Rotors under Persistent Uncertainties

Chen Meili *, *Wang Yuan*

College of Aerospace Engineering, Nanjing University of Aeronautics and Astronautics, Nanjing 210016, P. R. China

(Received 1 July 2017; revised 23 December 2017; accepted 10 January 2018)

Abstract: Nonlinear dynamic inversion (NDI) has been applied to the control law design of quad-rotors mainly thanks to its good robustness and simplicity of parameter tuning. However, the weakness of relying on accurate model greatly restrains its application on quad-rotors, especially nano quad-rotors (NQRs). NQRs are easy to be influenced by uncertainties such as model uncertainties (mainly from complicated aerodynamic interferences, strong coupling in roll-pitch-yaw channels and inaccurate aerodynamic prediction of rotors) and external uncertainties (mainly from winds or gusts), particularly persistent ones. Therefore, developing accurate model for altitude and attitude control of NQRs is difficult. To solve this problem, in this paper, an improved nonlinear dynamic inversion (INDI) method is developed, which can reject the above-mentioned uncertainties by estimating them and then counteracting in real time using linear extended state observer (LESO). Comparison with the traditional NDI (TNDI) method was carried out numerically, and the results show that, in coping with persistent uncertainties, the INDI-based method presents significant superiority.

Key words: nonlinear dynamic inversion; extended state observer; nano quad-rotor; uncertainties rejection; altitude control; attitude control

CLC number: V249.1 **Document code**: A **Article ID**: 1005-1120(2018)03-0483-11

Nomenclature

$(\varphi,\theta,\psi)^{\mathrm{T}}$ /rad	Euler angle
$(p,q,r)^{\mathrm{T}}$ /(rad·s^{-1})	Angular velocity
T_r /N	Lift
u_2/(N·m)	Roll torque
u_3/(N·m)	Pitch torque
u_4/(N·m)	Yaw torque
I_x /(kg·m^2)	Roll inertial
I_y /(kg·m^2)	Pitch inertial
I_z /(kg·m^2)	Yaw inertial
l /m	Lever
$(\varphi_{\mathrm{d}},\theta_{\mathrm{d}},\psi_{\mathrm{d}})^{\mathrm{T}}$ /rad	Desired Euler angle
f_φ /(rad·s^{-2})	Unknown nonlinear part of roll angle subsystem
f_θ /(rad·s^{-2})	Unknown nonlinear part of pitch angle subsystem
f_ψ /(rad·s^{-2})	Unknown nonlinear part of yaw angle subsystem
g_φ /(kg·m)	Given-part of roll angle equation
g_θ /(kg·m)	Given-part of pitch angle equation
g_ψ /(kg·m^2)	Given-part of yaw angle equation
$\tilde{f}_\varphi$ /(rad·s^{-2})	Estimate of f_φ
$\tilde{f}_\theta$ /(rad·s^{-2})	Estimate of f_θ
$\tilde{f}_\psi$ /(rad·s^{-2})	Estimate of f_ψ

0 Introduction

During the past decades, many researchers have focused on various kinds of control methods, especially the ones rely on specific mathematical models, to improve the control of quad-rotors. For example, reduced model based PID and linear quadratic (LQ) methods[1-3], accurate model based nonlinear feedback linearization method[4-7], and

* Corresponding author, E-mail address: meilil_3645@nuaa.edu.cn.

How to cite this article: Chen Meili, Wang Yuan. An improved nonlinear dynamic inversion method for altitude and attitude control of nano quad-rotors under persistent uncertainties[J]. Trans. Nanjing Univ. Aero. Astro., 2018,35(3):483-493. http://dx.doi.org/10.16356/j.1005-1120.2018.03.483

nonlinear dynamic inversion[8] were developed. Some other methods were proposed for allowing partial model information to vary within certain range[9-10]. Though there are some methods relying on no detailed model[11-12], they are quit tedious in design process.

Only a few works have discussed the flight of ordinary-sized and micro-sized quad-rotors under external uncertainties using the above mentioned methods[12-17]. In addition, their mechanisms on disturbances rejection mainly focus on enhancing the robustness of the control system and resisting instantaneous uncertainties, but they take no consideration on persistent ones, which may be a usual case in reality.

Therefore, according to the above discussion, in the design of control system of nano quad-rotors (NQRs), two problems need to be addressed under persistent uncertainties. Firstly, controllers should have good robustness. Secondly, controllers should not rely on accurate model. To solve those problems, in this paper, a robust INDI method based on the TNDI method and the linear extended state observer (LESO) is developed to design the altitude and attitude control law for NQRs. As known to all, NDI-based controller has some advantages[18], for instance, its structure is very simple, only a few parameters need to be tuned and their determination is very simple according to the bandwidth of state variables. Generally, the control effect in the TNDI method completely depends on the accuracy of the model. As discussed above, the internal and external uncertainties cannot be modeled precisely or some even cannot be modeled. To overcome this drawback of TNDI, the LESO is introduced into NDI to estimate the uncertainties using only input and output data of the control system. Hence, the uncertain dynamics in the controllers can be predicted and then counteracted. To show the superiority of the INDI-based method, a numerical comparison with TNDI was carried out.

1 Structure of Altitude and Attitude-Control Systems for NQRs

Before modeling NQRs, two coordinates (inertial and body), some forces, moments and geometrical parameters are introduced first, as shown in Fig. 1.

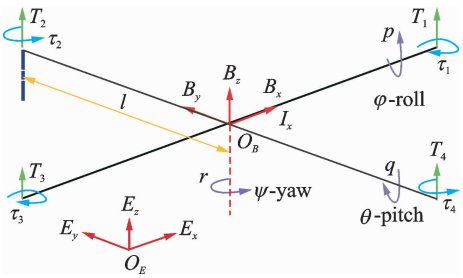

Fig. 1 Coordinates description of NQRs

In Fig. 1, $O_E E_x E_y E_z$ represents the inertial coordinate, in which E_x and E_y are on the horizontal plane and E_x is perpendicular to E_y, E_z is perpendicular to the horizontal determined by the right-hand rule. $O_B B_x B_y B_z$ represents the body coordinate centered at the center of gravity of the NQRs. B_x is the normal flight orientation, B_y is positive to starboard in the horizontal plane and B_z is orthogonal to the plane $B_x O_B B_y$.

The nonlinear movement equations of NQRs-without uncertainties are expressed as

$$\begin{cases} \dot{\boldsymbol{P}} = \boldsymbol{v} \\ \dot{\boldsymbol{v}} = g \cdot \boldsymbol{e}_z - \dfrac{1}{m}\boldsymbol{R}(\boldsymbol{\Theta}) \cdot T_r \cdot \boldsymbol{e}_z \\ \dot{\boldsymbol{\Theta}} = \boldsymbol{K}(\boldsymbol{\Theta}) \cdot \boldsymbol{\omega} \\ \dot{\boldsymbol{\omega}} = \boldsymbol{I}^{-1}(-\boldsymbol{\omega} \times \boldsymbol{I}\boldsymbol{\omega} + \tau) \end{cases} \tag{1}$$

where $\boldsymbol{P}, \boldsymbol{v} \in \mathbf{R}^3$ represent position and velocity of NQRs in inertial frame, respectively, m and g represent mass of NQRs and gravitational constant, respectively, $\boldsymbol{\omega} = [p, q, r]^{\mathrm{T}} \in \mathbf{R}^3$ is angular velocity in body coordinate, $\boldsymbol{\Theta} = [\varphi, \theta, \psi]^{\mathrm{T}} \in \mathbf{R}^3$ is Euler angle in inertial coordinate, T and τ are the total force and moment act on the frame of NQRs, $\boldsymbol{e}_z = [0, 0, 1]^{\mathrm{T}}$ is a vector along E_z, and $\boldsymbol{I} = \mathrm{diag}(I_x, I_y, I_z)$ is the moment of inertial matrix. The rotation matrix $\boldsymbol{R}(\boldsymbol{\Theta})$, which transforms a vector from inertial coordinate to body coordinate, has an expression as

$$\boldsymbol{R}(\boldsymbol{\Theta})=\begin{bmatrix}\cos\theta\cos\psi & -\cos\varphi\sin\psi+\sin\varphi\cos\psi & \sin\varphi\sin\psi+\cos\varphi\sin\theta\cos\psi\\ \cos\theta\cos\psi & \cos\varphi\sin\psi+\sin\varphi\cos\psi & -\sin\varphi\sin\psi+\cos\varphi\sin\theta\cos\psi\\ -\sin\theta & \sin\varphi\cos\theta & \cos\varphi\cos\theta\end{bmatrix}$$

And the attitude kinematic matrix $\boldsymbol{K}(\boldsymbol{\Theta})$ is defined as

$$\boldsymbol{K}(\boldsymbol{\Theta})=\begin{bmatrix}1 & \sin\varphi\tan\theta & \cos\varphi\tan\theta\\ 0 & \cos\varphi & -\sin\varphi\\ 0 & \sin\varphi\sec\theta & \cos\varphi\sec\theta\end{bmatrix}$$

During the flight, NQRs may be influenced by internal and external uncertainties, for example, the vibration derives from the asymmetry of eccentricity of rotor shafts, asymmetry of rotor blades and asymmetry of frame, winds and gusts and so forth. Hence, taking consideration of uncertainties, Eq. (2) yields the altitude and attitude movement equations of NQRs, shown as

$$\begin{cases}\ddot{h}=-g+\dfrac{T_r+\Delta T_r}{m}\cos\varphi\cos\theta\\ \dot{\boldsymbol{\Theta}}=\boldsymbol{K}(\boldsymbol{\Theta})\boldsymbol{\omega}\\ \dot{\boldsymbol{\omega}}=\boldsymbol{f}_{pqr}+\boldsymbol{V}\end{cases}\tag{2}$$

where

$$\boldsymbol{f}_{pqr}=\begin{bmatrix}f_p\\ f_q\\ f_r\end{bmatrix}=\begin{bmatrix}\dfrac{I_y-I_z}{I_x}qr\\ \dfrac{I_z-I_x}{I_y}pr\\ \dfrac{I_z-I_x}{I_z}pq\end{bmatrix}+\begin{bmatrix}\dfrac{l}{I_x} & 0 & 0\\ 0 & \dfrac{l}{I_y} & 0\\ 0 & 0 & \dfrac{1}{I_z}\end{bmatrix}\begin{bmatrix}\Delta\tau_{\text{roll}}\\ \Delta\tau_{\text{pitch}}\\ \Delta\tau_{\text{yaw}}\end{bmatrix}+\begin{bmatrix}\Delta d_{\text{roll}}\\ \Delta d_{\text{pitch}}\\ \Delta d_{\text{yaw}}\end{bmatrix}\tag{3}$$

$$\boldsymbol{V}=\begin{bmatrix}V_1\\ V_2\\ V_3\end{bmatrix}=\begin{bmatrix}\dfrac{l}{I_x} & 0 & 0\\ 0 & \dfrac{l}{I_y} & 0\\ 0 & 0 & \dfrac{1}{I_z}\end{bmatrix}\begin{bmatrix}\tau_{\text{roll}}\\ \tau_{\text{pitch}}\\ \tau_{\text{yaw}}\end{bmatrix}\tag{4}$$

In Eq. (4), $[\Delta\tau_{\text{roll}},\Delta\tau_{\text{pitch}},\Delta\tau_{\text{yaw}}]^{\mathrm{T}}$ represents the movement disturbances and $[\Delta d_{\text{roll}},\Delta d_{\text{pitch}},\Delta d_{\text{yaw}}]^{\mathrm{T}}$ represents the internal uncertainties.

2 Brief Introduction of LESO

2.1 Fundamental theory of high-order LESO

The $(n+1)$th-order LESO is mainly used to observe nth-order control system. Take the following nth-order linear affine differential system as an example

$$\Sigma:\begin{cases}\dot{x}_1=x_2\\ \vdots\\ \dot{x}_n=f(x_1,\cdots,x_n,t)+b\cdot u\\ y=x_1\end{cases}\tag{5}$$

where u and y are input and output of Σ, respectively, and $b>0$. Assume that $f(x_1,\cdots,x_n,t)$ is bounded and differentiable and its derivative with respect to t is $n(x_1,\cdots,x_n,t)$. Also bounded, this assumption is always reasonable in the control of quad-rotors. Then system Σ can be extended as the following formation

$$\Sigma_{\text{extend}}:\begin{cases}\dot{x}_1=x_2\\ \vdots\\ \dot{x}_n=x_{n+1}+b\cdot u\\ \dot{x}_{n+1}=n(x_1,\cdots,x_n,t)\\ y=x_1\end{cases}\tag{6}$$

Using a linear state observer[19-21] to observe Σ_{extend} yields

$$\Sigma_{\text{ESO}}:\begin{cases}e=z_1-y\\ \dot{z}_1=z_2-\sigma_1\cdot e\\ \vdots\\ \dot{z}_n=z_{n+1}-\sigma_n\cdot e+b\cdot u\\ \dot{z}_{n+1}=-\sigma_{n+1}\cdot e\\ y=x_1\end{cases}\tag{7}$$

The above system Σ_{ESO} is the so-called LESO. Thus, z_i tracks $x_i(i=1,\cdots,n)$ and z_{n+1} estimates $f(x_1,\cdots,x_n,t)$.

2.2 Stability analysis of LESO

In this part, stability of the $(n+1)$th-order LESO is proved. Firstly, rewrite Eq. (7) as the following formation

$$\dot{\boldsymbol{X}}=\boldsymbol{A}\cdot\boldsymbol{X}+\boldsymbol{B}_u\cdot u+\boldsymbol{B}_n\cdot n\tag{8}$$

where

$$\boldsymbol{X}=[x_1,\cdots,x_n]^{\mathrm{T}}$$

$$\boldsymbol{A}=\begin{bmatrix}0 & 1 & 0 & \cdots & 0 & 0\\ 0 & 0 & 1 & \cdots & 0 & 0\\ \vdots & \vdots & \vdots & \ddots & \vdots & \vdots\\ 0 & 0 & 0 & \cdots & 0 & 1\\ 0 & 0 & 0 & \cdots & 0 & 0\end{bmatrix}$$

$$\boldsymbol{B}_u=\begin{bmatrix}0\\0\\\vdots\\b\\0\end{bmatrix},\ \boldsymbol{B}_n=\begin{bmatrix}0\\0\\\vdots\\0\\1\end{bmatrix} \tag{9}$$

And Eq. (8) can be rewritten as

$$\dot{\boldsymbol{Z}}=\boldsymbol{A}\cdot\boldsymbol{Z}+\boldsymbol{B}_u\cdot u+\boldsymbol{B}_E\cdot\boldsymbol{E} \tag{10}$$

where

$$\boldsymbol{Z}=[z_1,\cdots,z_{n+1}]^{\mathrm{T}},\boldsymbol{e}_i=z_i-x_i\quad i=1,\cdots,n+1$$

$$\boldsymbol{E}=[\boldsymbol{e}_1,\boldsymbol{e}_2,\cdots,\boldsymbol{e}_n,\boldsymbol{e}_{n+1}]^{\mathrm{T}}$$

$$\boldsymbol{B}_E=\begin{bmatrix}-\sigma_1&0&0&\cdots&0&0\\-\sigma_2&0&0&\cdots&0&0\\\vdots&\vdots&\vdots&\ddots&\vdots&\vdots\\-\sigma_n&0&0&\cdots&0&0\\-\sigma_{n+1}&0&0&\cdots&0&0\end{bmatrix} \tag{11}$$

Hence, subtracting Eq. (9) from Eq. (11) yields

$$\dot{\boldsymbol{E}}=\boldsymbol{A}_E\cdot\boldsymbol{E}-\boldsymbol{B}_n\cdot n=\begin{bmatrix}-\sigma_1&1&0&\cdots&0&0\\-\sigma_2&0&1&\cdots&0&0\\\vdots&\vdots&\vdots&\ddots&\vdots&\vdots\\-\sigma_n&0&0&\cdots&0&1\\-\sigma_{n+1}&0&0&\cdots&0&0\end{bmatrix}\cdot\boldsymbol{E}-\begin{bmatrix}0\\0\\\vdots\\0\\1\end{bmatrix}\cdot n \tag{12}$$

Since $n=n(x_1,\cdots,x_n,t)$ is a bounded function as defined before, the $(n+1)$th-order LESO is bounded-input bounded-output (BIBO) if the roots of the characteristic polynomial of $\boldsymbol{A}_E$, shown as

$$\lambda(p)=p^{n+1}+\sigma_1 p^n+\sigma_2 p^{n-1}+\cdots+\sigma_n p+\sigma_{n+1} \tag{13}$$

are all in the left half plane. Thus, stability of the $(n+1)$th-order LESO is proved.

3 Design of Altitude Control Law

3.1 Design of NDI-based altitude control law

In this part, an altitude control law based on NDI is derived. During the motion of NQR, $\cos\varphi\approx1$, $\cos\theta\approx1$ and ΔT_r is uncertain. Hence, in NDI, Eq. (2) is usually rewritten as

$$\ddot{h}=-g+\frac{T_r}{m} \tag{14}$$

Denoting $f_z=-g$ and $g_z=\dfrac{1}{m}$ yields

$$\ddot{h}=f_z+g_z\cdot T_r \tag{15}$$

Solving the above equation yields the desired thrust, that is

$$T_{rd}=g_z^{-1}\cdot(\ddot{h}-f_z) \tag{16}$$

where $\ddot{h}$ can be obtained by employing PD control law.

Assume that h_d represents the desired trajectory of altitude and h represents the feedback trajectory of altitude, then the tracking error $e=h_d-h$ satisfies the following equation

$$\ddot{e}+k_d\dot{e}+k_p e=0$$

Therefore, by substituting $e=h_d-h$ into the above equation, expression of $\ddot{h}$ can be obtained as

$$\ddot{h}=\ddot{h}_d+k_d(\dot{h}_d-\dot{h})+k_p(h_d-h)$$

According to the above analysis, the overall structure of the altitude control system based on NDI is shown in Fig. 2.

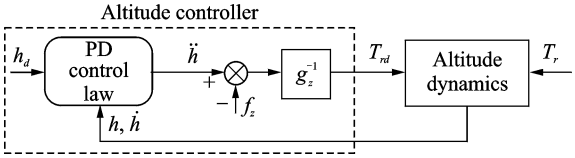

Fig. 2 Structure of the altitude control system based on NDI for NQRs

3.2 INDI-based altitude control law improved using LESO

In NDI, ΔT_r is ignored, which always results in the low accuracy of the counteraction of nonlinear terms since ΔT_r usually affects the quality of the controller and the robustness of the system. In this part, ΔT_r is taken into account by taking advantage of LESO. In Eq. (16), considering the disturbance ΔT_r and putting it into f_z yields

$$\begin{cases}\ddot{h}=\bar{f}_z+g_z\cdot T_r\\\bar{f}_z=-g+\dfrac{\Delta T_r}{m}\end{cases} \tag{17}$$

By denoting $x_1=h$, $x_2=\dot{h}$, $x_3=\bar{f}_z$, $\dot{x}_3=n_z$, the above equation can be rewritten as the formation of state space equation

$$\begin{cases}\dot{x}_1=x_2\\\dot{x}_2=x_3+g_z\cdot T_r\\\dot{x}_3=n_z\\y=x_1\end{cases} \tag{18}$$

Using third-order LESO to observe the above extended system yields

$$\begin{cases} e = y - z_1 \\ \dot{z}_1 = z_2 - \rho_1 \cdot e \\ \dot{z}_2 = z_3 - \rho_2 \cdot e + g_z \cdot T_r \\ \dot{z}_3 = -\rho_3 \cdot e \end{cases} \tag{19}$$

Therefore, z_1 tracks x_1, z_2 tracks x_2, and z_3 estimates $\overline{f}_z$.

By using LESO to make the estimation, the control scheme changes into the following pattern, as shown in Fig. 3.

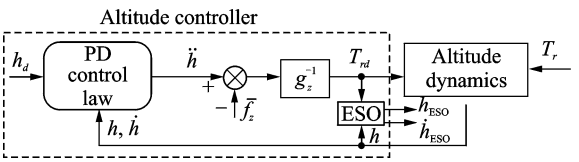

Fig. 3 Structure of the INDI-based altitude control system improved using LESO for NQRs

A direct method to verify the correctness of this theory is to check the agreement between $(h, \dot{h})$ and $(h_{ESO}, \dot{h}_{ESO})$, which will be checked in simulations hereinafter.

3.3 Parameter tuning principles of altitude control

On one hand, in Eq. (18), following the relationship between k_d and k_p can ensure the disappearance of overshoot

$$k_p = \lambda^2, k_d = 2\lambda \quad \lambda > 0 \tag{20}$$

On the other hand, to derive the parameters of the third-order LESO, transfer function of Eq. (22) from z_3 to y and T_r needs to be obtained, shown as

$$z_3 = \frac{\rho_3^z}{s^3 + \rho_1^z \cdot s^2 + \rho_2^z \cdot s + \rho_3^z}(s^2 \cdot y - g_z \cdot T_r) \tag{21}$$

According to Ref. [22], ρ_1^z, ρ_2^z and ρ_3^z can be determined as

$$\rho_1^z = 3\omega_z, \rho_2^z = 3\omega_z^2, \rho_3^z = \omega_z^3 \quad \omega_z > 0 \tag{22}$$

where ω_z is called bandwidth of roll angular velocity channel and thus the transfer function turns into

$$z_3 = \frac{\omega_z^3}{(s + \omega_z)^3}(s^2 \cdot y - g_z \cdot T_r) \tag{23}$$

Therefore, in the altitude control system, only one parameter needs to be tuned since λ can be determined empirically, for example, its recommended value can be 1 or 2.

4 Design of Attitude Control Law

4.1 Design of NDI-based attitude control law

To derive the Euler angle control law, Eq. (2) needs to be addressed.

Denote

$$\boldsymbol{T} = \begin{bmatrix} 1 & \sin\varphi\tan\theta & \cos\varphi\tan\theta \\ 0 & \cos\varphi & -\sin\varphi \\ 0 & \sin\varphi\sec\theta & \cos\varphi\sec\theta \end{bmatrix} \tag{24}$$

Hence, Eq. (2) can be rewritten as

$$\begin{bmatrix} \dot{\varphi} \\ \dot{\theta} \\ \dot{\psi} \end{bmatrix}_d = \boldsymbol{T} \begin{bmatrix} p \\ q \\ r \end{bmatrix}_d \tag{25}$$

Then the desired angular velocity and the input of angular velocity controller can be obtained as

$$\begin{bmatrix} p \\ q \\ r \end{bmatrix}_d = \boldsymbol{T}^{-1} \begin{bmatrix} \dot{\varphi} \\ \dot{\theta} \\ \dot{\psi} \end{bmatrix}_d \tag{26}$$

where $[\dot{\varphi}, \dot{\theta}, \dot{\psi}]_d^{\mathrm{T}}$ can be calculated by

$$\begin{bmatrix} \dot{\varphi} \\ \dot{\theta} \\ \dot{\psi} \end{bmatrix}_d = \boldsymbol{K}_1 \left\{ \begin{bmatrix} \varphi \\ \theta \\ \psi \end{bmatrix}_d - \begin{bmatrix} \varphi \\ \theta \\ \psi \end{bmatrix} \right\} \tag{27}$$

and $[\varphi, \theta, \psi]^{\mathrm{T}}$ is the real-time feedback value of attitude and $\boldsymbol{K}_1 = \mathrm{diag}(\omega_1, \omega_1, \omega_1)$.

After deriving the Euler angle controller, the angular velocity controller needs to be designed.

In Eqs. (4), (5), denote

$$\boldsymbol{R} = \begin{bmatrix} \dfrac{l}{I_x} & 0 & 0 \\ 0 & \dfrac{l}{I_y} & 0 \\ 0 & 0 & \dfrac{1}{I_z} \end{bmatrix} \tag{28}$$

And rewrite Eq. (4) as

$$\begin{bmatrix} \dot{p} \\ \dot{q} \\ \dot{r} \end{bmatrix}_d = \begin{bmatrix} f_p \\ f_q \\ f_r \end{bmatrix} + \boldsymbol{R} \begin{bmatrix} \tau_{\mathrm{roll}} \\ \tau_{\mathrm{pitch}} \\ \tau_{\mathrm{yaw}} \end{bmatrix}_d \tag{29}$$

Then the desired virtual input can be solved, shown as

$$\begin{bmatrix} \tau_{\mathrm{roll}} \\ \tau_{\mathrm{pitch}} \\ \tau_{\mathrm{yaw}} \end{bmatrix}_d = \boldsymbol{R}^{-1} \left\{ \begin{bmatrix} \dot{p} \\ \dot{q} \\ \dot{r} \end{bmatrix}_d - \begin{bmatrix} f_p \\ f_q \\ f_r \end{bmatrix} \right\} \tag{30}$$

where $[\dot{p},\dot{q},\dot{r}]_d^{\mathrm{T}}$ can be calculated by

$$\begin{bmatrix}\dot{p}\\ \dot{q}\\ \dot{r}\end{bmatrix}_d = \boldsymbol{K}_2\left\{\begin{bmatrix}p\\ q\\ r\end{bmatrix}_d - \begin{bmatrix}p\\ q\\ r\end{bmatrix}\right\} \tag{31}$$

The desired angular velocity $[p,q,r]_d^{\mathrm{T}}$ has been obtained in above, $[p,q,r]^{\mathrm{T}}$ is the real-time feedback value of angular velocity, and $\boldsymbol{K}_2 = \mathrm{diag}(\omega_2,\omega_2,\omega_2)$.

According to the above analysis, the overall structure of the attitude control system is shown in Fig. 4.

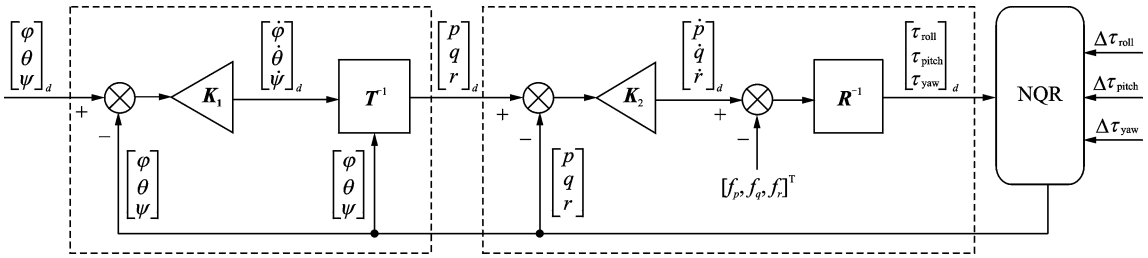

Fig. 4 Structure of the NDI-based attitude control system for NQRs

The above analysis also clearly shows the biggest weakness of TNDI, that is, the robustness and quality of the attitude controller depends on the modeling precision of $[f_p,f_q,f_r]^{\mathrm{T}}$. Ref. [19] has proved that TNDI can address the case with small perturbations in $[f_p,f_q,f_r]^{\mathrm{T}}$; while with large perturbations in $[f_p,f_q,f_r]^{\mathrm{T}}$, for instance, in the existence of persistent external uncertainties, the TNDI cannot perform well. In most cases, the nonlinearity of the model can be counteracted completely only when the nonlinear terms $[f_p,f_q,f_r]^{\mathrm{T}}$ are accurate enough, which restrains the application of TNDI.

4.2 INDI-based attitude control law improved using LESO

To overcome the weakness discussed above, LESO is used to estimate the accurate and real time value of $[f_p,f_q,f_r]^{\mathrm{T}}$. Hence, it is necessary to introduce the LESO first and then give the improved control law based on LESO. In this paper, only the estimation of f_p using LESO is introduced as f_q and f_r are very similar.

In the first equation of Eq. (2), denote that

$$\begin{cases}x_1 = p\\ x_2 = f_p\\ \dot{x}_2 = g_p\end{cases} \tag{32}$$

Hence, the roll angular velocity system is rewritten as

$$\begin{cases}\dot{x}_1 = x_2 + \dfrac{l}{I_x}\cdot\tau_{\mathrm{roll}}\\ \dot{x}_2 = g_p\\ y = x_1\end{cases} \tag{33}$$

Using second-order LESO to observe the above extended system yields

$$\begin{cases}e = y - z_1\\ \dot{z}_1 = z_2 - \rho_1^p\cdot e + \dfrac{l}{I_x}\cdot\tau_{\mathrm{roll}}\\ \dot{z}_2 = -\rho_2^p\cdot e\end{cases} \tag{34}$$

Therefore, z_1 tracks p and z_2 estimates f_p.

By employing LESO to conduct the estimation, the control scheme changes into the following pattern, as shown in Fig. 5.

A direct method to verify the correctness of this theory is to check the agreement between $[p,q,r]^{\mathrm{T}}$ and $[p_{\mathrm{ESO}},q_{\mathrm{ESO}},r_{\mathrm{ESO}}]^{\mathrm{T}}$, which will be checked in simulations hereinafter.

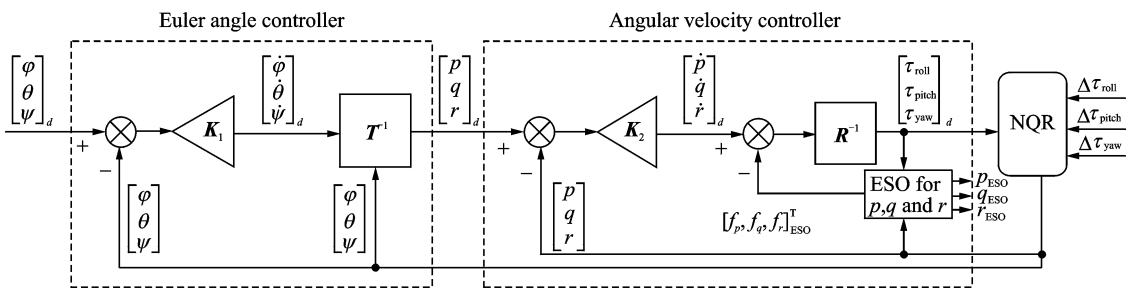

Fig. 5 Structure of the INDI-based attitude control system using LESO for NQRs

4.3 Parameter tuning principles of attitude control

In one way, in the attitude controller, the parameters ω_1 and ω_2 together determine both the tracking precision and the response speed of the system. Since the response speed of angular velocity is much faster than the one of Euler angle, thus, the two parameters usually satisfy the following relationship[19]

$$\omega_2 = n \cdot \omega_1 \quad n = 3\text{—}5 \tag{35}$$

Put another way, in the LESO, ρ_1^p and ρ_2^p determine the tracking precision and speed, too small value may cause a bad tracking performance and too large value may result in divergence of the system. Taking the transfer function of Eq. (34) yields

$$z_2 = \frac{\rho_2^p}{s^2 + \rho_1^p \cdot s + \rho_2^p}(s \cdot y - \frac{l}{I_x} \cdot \tau_{\text{roll}}) \tag{36}$$

Notice that it is a typical second order system and to avoid the overshoot, Gao[22] also recommended a method to determine ρ_1^p and ρ_2^p, shown as

$$\rho_1^p = 2\omega_p, \rho_2^p = \omega_p^2 \quad \omega_p > 0 \tag{37}$$

where ω_p is called bandwidth of roll angular velocity channel and thus, the transfer function turns into

$$z_2 = \frac{\omega_p^2}{(s + \omega_p)^2}(s \cdot y - \frac{l}{I_x} \cdot \tau_{\text{roll}}) \tag{38}$$

Hence, in each angular velocity channel (roll, pitch and yaw), only two parameters need to be determined.

5 Numerical Validation

Two numerical simulations were conducted. The first one aims to demonstrate the superiority of INDI compared with TNDI in the existence of model uncertainties; and the second one in turn demonstrates the superiority of INDI compared with TNDI in the existence of both external uncertainties and model uncertainties.

5.1 Variables and parameters

The parameters of the NQR used in the simulations are listed in Table 1.

The initial conditions are given as

$$\begin{cases} h_0 = 0 \\ (\varphi, \theta, \psi)_0^{\mathrm{T}} = (0,0,0)^{\mathrm{T}} \\ (p, q, r)_0^{\mathrm{T}} = (0,0,0)^{\mathrm{T}} \end{cases} \tag{39}$$

Table 1 Parameters of NQR

Parameter	m /g	g /(m·s^{-2})	l /mm	I_x /(kg·m^2)	I_y /(kg·m^2)	I_z /(kg·m^2)	b	k
Value	43	9.81	35	1.916×10^{-5}	1.916×10^{-5}	2.781×10^{-5}	2.478×10^{-8}	1.193×10^{-9}

The desired altitude and attitude trajectories are given as

$$\begin{cases} h_d(t) = 4 + 3\sin t(m) \\ [\varphi_d, \theta_d, \psi_d]^{\mathrm{T}} = [0.1\ \text{rad}, 0.1\ \text{rad}, 0.1\ \text{rad}]^{\mathrm{T}} \end{cases} \tag{40}$$

Values of parameters of NDI controllers are shown in Table 2. Values of parameters of LESOs are shown in Table 3.

Table 2 Values of parameters of NDI controllers

Channel	Altitude	Roll	Pitch	Yaw
Value	$r = 1$	$\omega_1 = 7$ $\omega_2 = 21$	$\omega_1 = 7$ $\omega_2 = 21$	$\omega_1 = 6$ $\omega_2 = 18$

Table 3 Values of parameters of LESOs

Parameter	ω_z	ω_p	ω_q	ω_r
Value	100	150	150	150

5.2 Case study: INDI vs. TNDI under low and high frequency uncertainties

In this part, low and high frequency uncertainties were considered together. Δd_{roll}, Δd_{pitch} and Δd_{yaw} were assumed to be the triangle functions including low and high frequency components. This assumption is reasonable since such uncertainties derive from many aspects, for instance, eccentricity of rotor shafts, asymmetry of both rotor blades and frame, body vibration on sensors, unstable voltage of circuit and larger ripple current, and they can be modeled and extended to the trigonometric series. Furthermore, there was an additional mass (8% of the mass of NQR) added on the NQR during its flight meanwhile. The figures of state variables and outputs of NQR are shown in Figs. 6—21.

Fig. 6, Fig. 7 and Fig. 14 show the simulation results in altitude control using the INDI-based and TNDI-based methods. Fig. 6 and Fig. 7 together depict the tracking results, and obviously

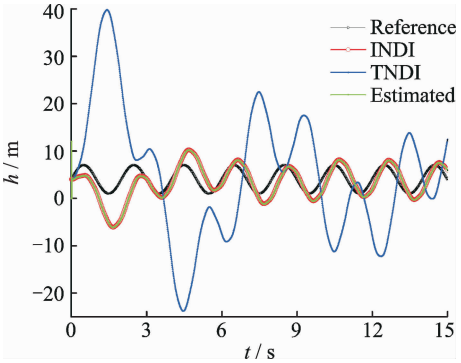

Fig. 6 Response of altitude

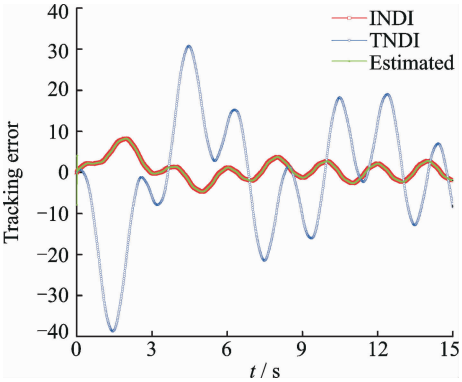

Fig. 7 Tracking error of altitude response

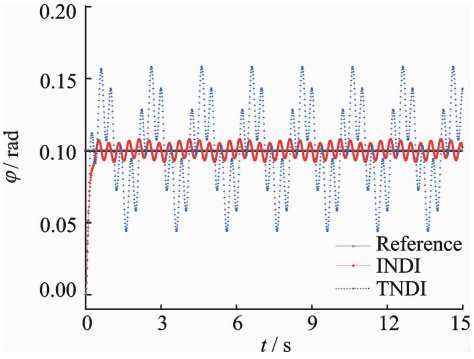

Fig. 8 Response of roll angle

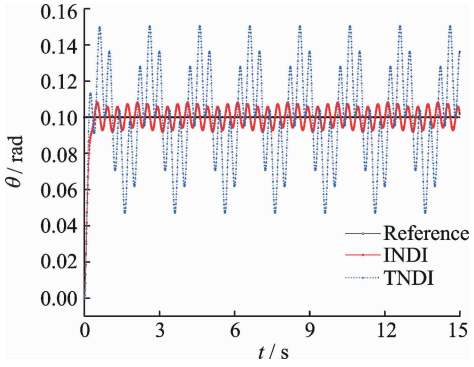

Fig. 9 Response of pitch angle

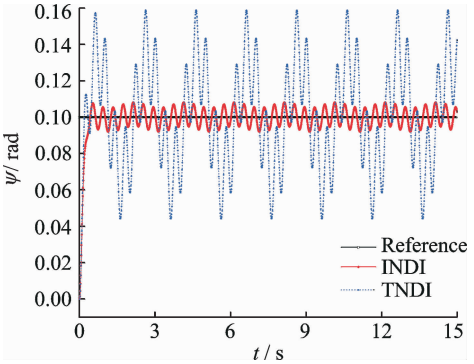

Fig. 10 Response of yaw angle

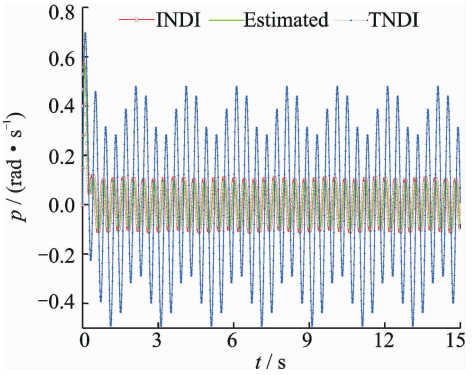

Fig. 11 Roll angular rate

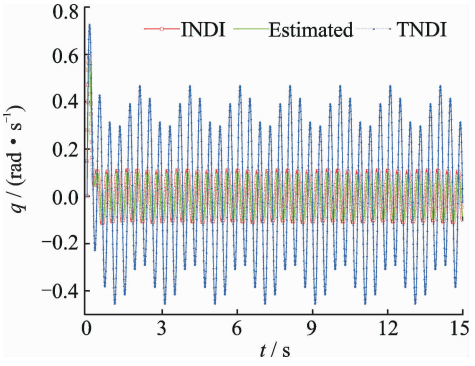

Fig. 12 Pitch angular rate

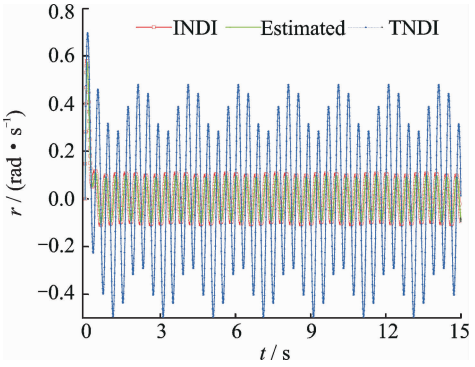

Fig. 13 Yaw angular rate

the tracking effect derived from the INDI-based method is much better (also acceptable) than the one from the TNDI-based method since the former one owns much higher accuracy. The correctness of the estimation obtained by LESO is also demonstrated in the three figures since the curves of the estimated state variables are overlapped with the ones of the real state variables.

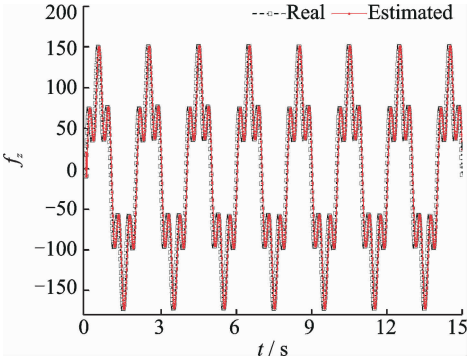

Fig. 14 Estimation of f_z by LESO

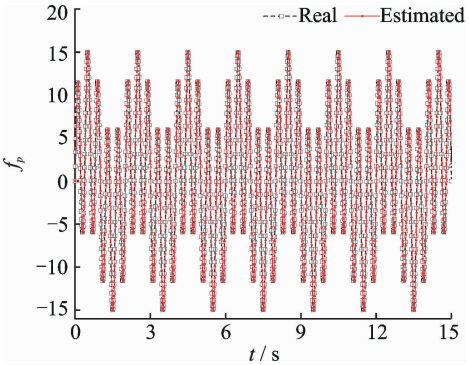

Fig. 15 Estimation of f_p by LESO

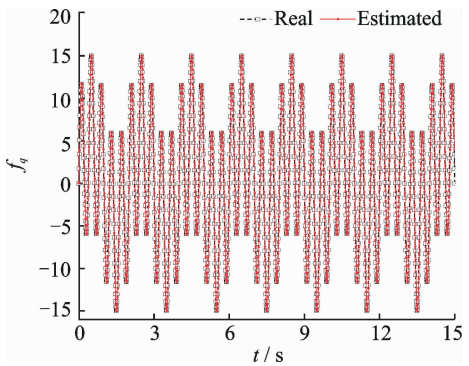

Fig. 16 Estimation of f_q by LESO

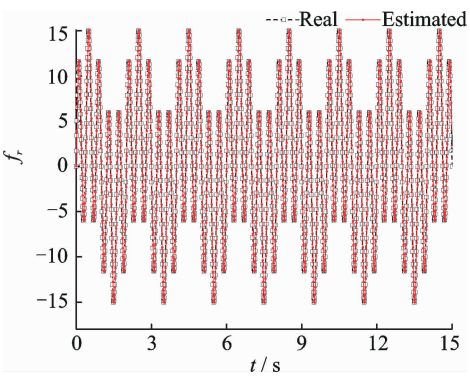

Fig. 17 Estimation of f_r by LESO

Figs. 8—10 show the results in attitude control using both methods. It is clear that the INDI-based method can still hold the attitude of the NQR steady even under persistent high/low frequency disturbances.

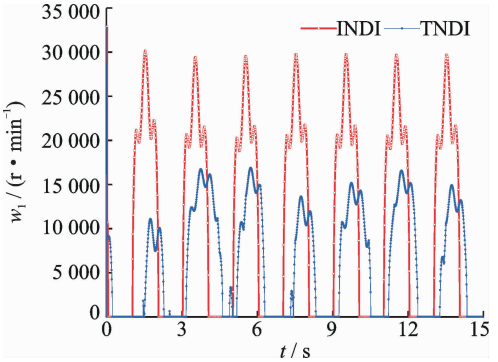

Fig. 18 Speed of rotor 1

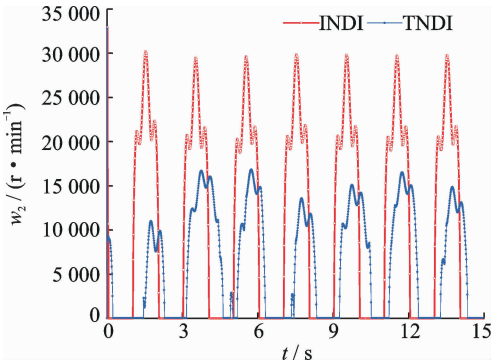

Fig. 19 Speed of rotor 2

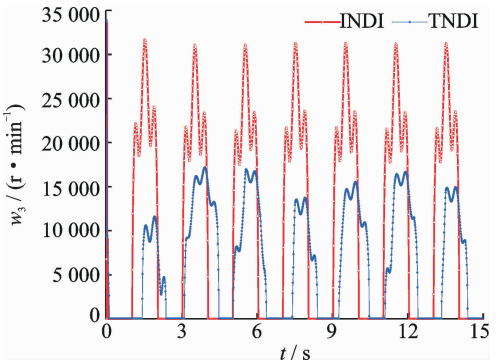

Fig. 20 Speed of rotor 3

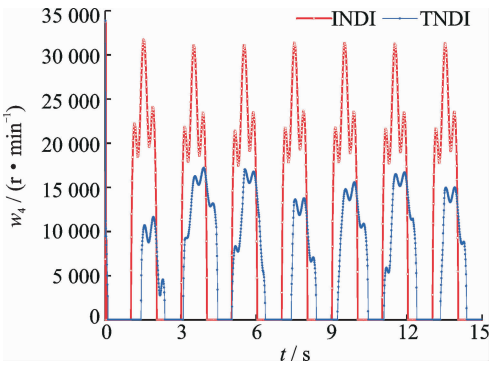

Fig. 21 Speed of rotor 4

Figs. 18—21 show the desired rotor speed of the NQR. Notice that the curves of the input variables in the TNDI-based method are much smoother than those in the INDI-based method. The reason is that, in TNDI uncertainties rejec-

tion mostly relies on the robustness of its controller. When uncertainties are added into the plant, the controller cannot make response to them, which results in the smooth curves. While situations are different in the INDI-based method since LESO has the ability to estimate uncertainties, and then counteract them in each time step, which results in the fluctuation of the curves of the input variables in INDI-based method. This also in turn explains why the INDI-based method has better tracking precision in both altitude and attitude controls.

6 Conclusions

An INDI-based method is developed to design the altitude and attitude control systems for NQRs. To solve the problem that TNDI relies heavily on accurate model of NQR, which is difficult to be obtained, and to retain the robustness of TNDI, the LESO is introduced into TNDI to estimate the model and external uncertainties and then counteract in real time. Comparison between simulation results of the two methods shows that the INDI-based method can reject the uncertainties better, and it does not rely on the accurate model, presenting significant superiority.

Acknowledgements

This work was supported by the Priority Academic Program Development of Jiangsu Higher Education Institutions (PAPD) and the Advanced Research Project of Army Equipment Development (No. 301020803).

References:

[1] SÁ R C, ARAÚJO A L, VARELA A T, et al. Construction and PID control for stability of an unmanned aerial vehicle of the type quadrotor[J]. Robotics Symposium and Competition, 2013, 10: 95-99.

[2] BOUABDALLAH S, NOTH A, SIEGWART R. PID vs LQ control techniques applied to an indoor microquadrotor[C]// IEEE/RSJ International Conference on Intelligent Robots and Systems. Sendai, Japan: IEEE, 2004, 3: 2451-2456.

[3] BOUABDALLAH S, SIEGWART R. Design and control of a miniature quadrotor[C]// Advances in Unmanned Aerial Vehicles. Netherlands: Springer, 2007, 33: 171-210.

[4] DIERKS T, JAGANNATHAN S. Output feedback control of a quadrotoruav using neural networks[J]. IEEE Transactions on Neural Networks, 2010, 21(1): 50-66.

[5] VOOS H. Nonlinear control of a quadrotor micro-UAV using feedback-linearization[C]// IEEE International Conference on Mechatronics. [S. l.]: IEEE, 2009: 1-6.

[6] HUA M D, HAMEL T, MORIN P, et al. A control approach for thrust-propelled underactuated vehicles and its application to VTOL drones[J]. IEEE Transactions on Automatic Control, 2009, 54(8): 1837-1853.

[7] DIKMEN I C, ARISOY A, TEMELTAS H. Attitude control of a quadrotor[C]// International Conference on Recent Advances in Space Technologies. Istanbul, Turkey: IEEE, 2009: 722-727.

[8] TIWARI S, PADHI R. DR-SNAC aided dynamic inversion controller for robust trajectory tracking of a micro-quadrotor[C]// AIAA Guidance, Navigation, and Control. Boston, MA: IEEE, 2013: 1-28.

[9] XU Y, TONG C, LI H. Flight control of a quadrotor under model uncertainties[J]. International Journal of Micro Air Vehicles, 2015, 7(1): 1-20.

[10] ZHAO B, XIAN B, ZHANG Y, et al. Nonlinear robust adaptive tracking control of a quadrotoruav via immersion and invariance methodology[J]. IEEE Transactions on Industrial Electronics, 2015, 62(5): 2891-2902.

[11] MADANI T, BENALLEGUE A. Control of a quadrotor mini-helicopter via full state Backstepping technique[C]// Proceedings of the IEEE Conference on Decision and Control. [S. l.]: IEEE, 2006: 1515-1520.

[12] KHEBBACHE H, TADJINE M. Robust fuzzy Backstepping sliding mode controller for a quadrotor unmanned aerial vehicle[J]. Control Engineering & Applied Informatics, 2013, 15(2): 3-11.

[13] LEE D, LIM H, KIM H J, et al. Adaptive image-based visual serving for an underactuatedquadrotorsystem[J]. Journal of Guidance Control & Dynamics, 2012, 35(4): 1335-1353.

[14] KUN D W, HWANG I. Linear matrix inequality-based nonlinear adaptive robust control of quadrotor [J]. Journal of Guidance Control & Dynamics, 2015: 1-13.

[15] BESNARD L, SHTESSEL Y B, Landrum B. Quadrotor vehicle control via sliding mode controller driven by sliding mode disturbance observer[J]. Journal of the Franklin Institute, 2012, 349(2): 658-684.

[16] ALEXIS K, NIKOLAKOPOULOS G, TZES A. Constrained-control of a quadrotor helicopter for trajectory tracking under wind-gust disturbances[C]// IEEE Mediterranean Electrotechnical Conference. Valletta, Malta: IEEE, 2010:1411-1416.

[17] MUÑOZ L E, CASTILLO P, SANAHUJA G, et al. Embedded robust nonlinear control for a four-rotor rotorcraft: Validation in real-time with wind disturbances[C]// IEEE/RSJ International Conference on Intelligent Robots and Systems. San Francisco, CA, USA: IEEE, 2011: 2682-2687.

[18] ITO D, GEORGIE J, VALASEK J, et al. Reentry vehicle flight controls design guidelines: Dynamic inversion[R]. NASA/TP 2002-210771, 2002.

[19] DOU J, KONG X, WEN B. Altitude and attitude active disturbance rejection controller design of a quadrotor unmanned aerial vehicle[J]. Proceedings of the Institution of Mechanical Engineers, Part G: Journal of Aerospace Engineering. 2016: DOI: 10.1177/0954410016660871.

[20] HAN J. From PID to active disturbance rejection control[J]. IEEE Transactions on Industrial Electronics, 2009, 56(3): 900-906.

[21] HAN J Q. Active disturbance rejection control technique the technique for estimating and compensating the uncertainties[M]. 1st ed. Beijing: National Defense Industry Press, 2008.

[22] GAO Z. Scaling and bandwidth-parameterization based controller tuning[C]// Proceedings of the 2003 American Control Conference. Denver, CO, USA: IEEE, 2003, 6: 4989-4996.

Ms. **Chen Meili** received her B. S. degree in navigation, guidance and control from Nanjing University of Aeronautics and Astronautics (NUAA), Nanjing, China, in 2005. From 2005 to present, she has been with the college of aerospace Engineering, NUAA, where she is currently an engineer of Key Laboratory of Fundamental Science for National Defense Advanced Design Technology of Flight Vehicle. Her research interest focuses on flight control of micro aircraft vehicles.

Mr. **Wang Yuan** received his B. S. degree in aircraft design from Nanjing University of Aeronautics and Astronautics (NUAA), Nanjing, China, in 2015. He is currently a Ph. D candidate. His research interest focuses on flight control and nonlinear control theories.

(Production Editor: Zhang Huangqun)